ORNL/TM-9705
Dist. Category UC-20

ORNL/TM--9705

DE86 002902

Fusion Energy Division

POTENTIAL MEASUREMENTS IN TANDEM MIRRORS

J. C. Glowienka

Date Published - November 1985

NOTICE This document contains information of a preliminary nature. It is subject to revision or correction and therefore does not represent a final report.

Prepared by the
OAK RIDGE NATIONAL LABORATORY
Oak Ridge, Tennessee 37831
operated by
MARTIN MARIETTA ENERGY SYSTEMS, INC.
for the
U.S. DEPARTMENT OF ENERGY
under Contract No. DE-AC05-84OR21400

CONTENTS

LIST OF FIGURES

1. INTRODUCTION

The U.S. mirror program is presently creating and sustaining a thermal barrier tandem mirror configuration. An integral part of the learning process is the ability to measure properties of the thermal barrier, the most obvious of which is the plasma potential in the barrier region relative to the plasma potential elsewhere along the device axis. This report addresses the current state of thermal barrier potential diagnostics, first by discussing the need for a thermal barrier, second by discussing the measurement techniques available, third by focusing on the techniques and on the ambiguities with published data, and fourth by describing diagnostic improvements under way.

2. MOTIVATION FOR A THERMAL BARRIER

A tandem mirror consists of two essential features: a long solenoidal mirror or central cell that provides radial confinement with a uniform magnetic field and end cells that provide axial plugging of the central cell by local electrostatic fields. Stability is also required, but this will not be discussed here. The essence of a tandem mirror confinement scheme is axial electrostatic confinement of central-cell ions with a potential in the end cell that is more positive than that in the central cell. This is done by intense neutral beam injection into the end-cell mirror, which raises the end-cell or plug density above the central-cell density. The potential in the plug goes as the Boltzmann relation,

$$\phi_p \propto T_e \ln(n_p/n_c) \ ,$$

where n_p is the plug density, n_c is the central-cell density, and T_e is the plug electron temperature. The axial potential profile of a conventional tandem mirror[1] is shown schematically in Fig. 1.

The plug potential ϕ_p is sustained by the neutral beams; ϕ_e is the central-cell potential that is achieved through any combination of neutral beam heating, ion cyclotron heating (ICH), and/or electron cyclotron heating (ECH); and ϕ_i is the ion confining potential. The intense neutral beam injection in the end cells also raises the electron temperature in the end cell. However, electrons are isothermal along field lines because the electron thermal conductivity is large, and, as a result, the power required to maintain the central-cell electron temperature at the plug electron temperature would seriously degrade the efficiency of a conventional tandem mirror reactor.

A recent innovation, the thermal barrier,[2] provides axial thermal isolation by the addition of a potential dip, ϕ_b, just inboard of the ion plugging potential, ϕ_p. The thermal barrier is formed by creating a sloshing ion population with neutral beams and a trapped hot electron population with ECH. The essential features of the axial potential profile in a thermal barrier tandem mirror are shown in Fig. 2.

The potential dip electrostatically confines electrons to the central cell; only those electrons with parallel energy greater than $e\phi_b$ at the barrier can leave the central cell. As a result, the axial electron confinement thermally isolates the colder central-cell electrons from the hotter plug electrons.

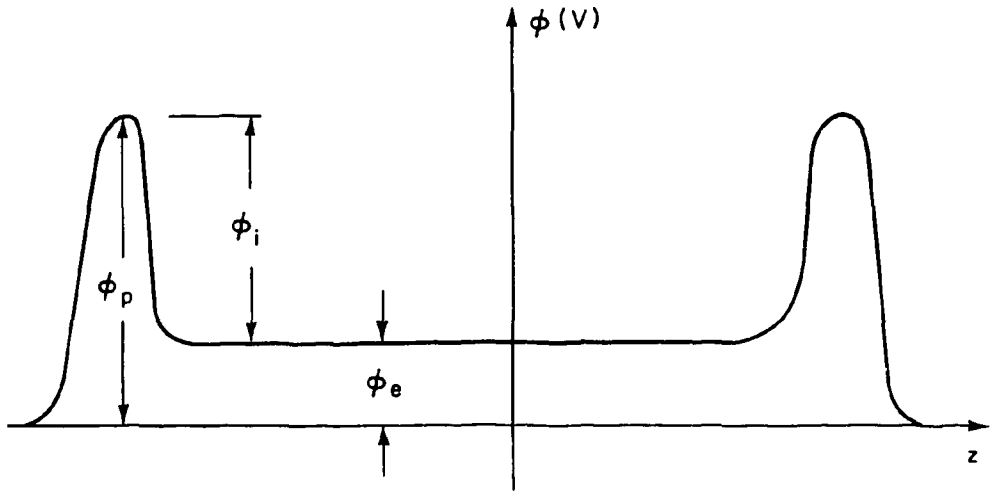

Fig. 1. Schematic diagram of the axial potential profile of a conventional tandem mirror.

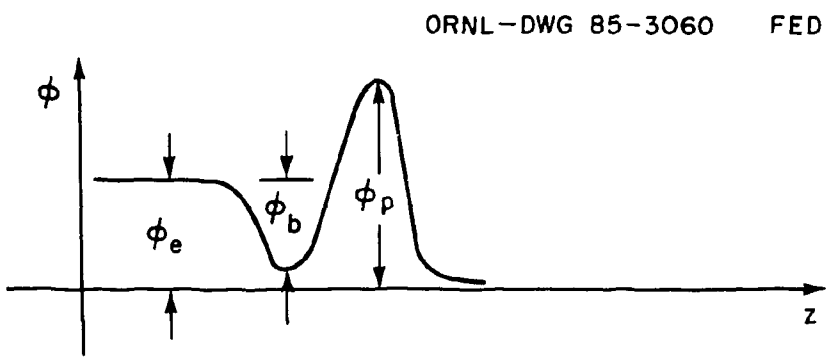

Fig. 2. Essential features of the axial potential profile of the thermal barrier tandem mirror.

3. POTENTIAL MEASUREMENT TECHNIQUES

Clearly the measurement of an axial and radial profile of the potential as a function of time is necessary to follow the development of the thermal barrier and axial plugging. Unfortunately, there are few diagnostics that can measure potential. Langmuir probes, end-loss analyzers (ELAs), and heavy-ion beam probes (HIBPs) provide the most direct measurements. In addition, spectroscopy can infer the direction and magnitude of a radial electric field by measuring the Doppler shift of emitted light. The standard for many years

had been the Langmuir probe; a large array could adequately provide potential profiles, but the energy density of present tandem mirror plasmas, particularly those with intense neutral beam injection, would destroy the probe. The HIBP can supply accurate, time-resolved radial potential profiles; TMX-U and Gamma 10 have operating systems. However, the present primary concern is the time-resolved axial potential profile because axial plugging is lost during interesting high-density experiments. The principal diagnostic used on mirror devices for axial potential information is an array of ELAs. An ELA is a passive diagnostic that is used to collect positive ions flowing out of the ends of mirror cells along field lines. The entrance aperture of the ELA defines the size of the flux tube observed.

Details of the design and operation of an ELA are found in an excellent paper by Molvik.[3] The ion current arises from ions that enter the loss cone of the mirror cell and are no longer confined. The mirror plasma remains stable if the loss-cone ions are replaced from the outside. As a result, the stable mirror plasma remains close to a Maxwellian distribution, $f(v) \propto \exp(-mv^2/2KT)$. Because a mirror-cell plasma develops a positive potential, ELA data are used to determine the peak potential and the average ion temperature[4] within the flux tube.

The basic piece of ELA data is a plot of $\ln(I)$ vs V, the natural logarithm of the measured end-loss ion current as a function of swept ion repeller voltage. One complete sweep can be obtained on the order of milliseconds, and with experiments that last several tens of milliseconds, time-resolved data have been obtained with ELAs. The characteristic shape of ELA data for a simple mirror is shown in Fig. 3.

The interpretation of the data is that the break in the curve or knee represents the peak plasma potential within the flux tube and that the inverse slope is proportional to the average ion temperature within the flux tube. This can be further understood by examining the total energy of a single particle. Within the plasma, the total energy of the particle is

$$E_T = 1/2mv^2 + e\phi + \mu B \ .$$

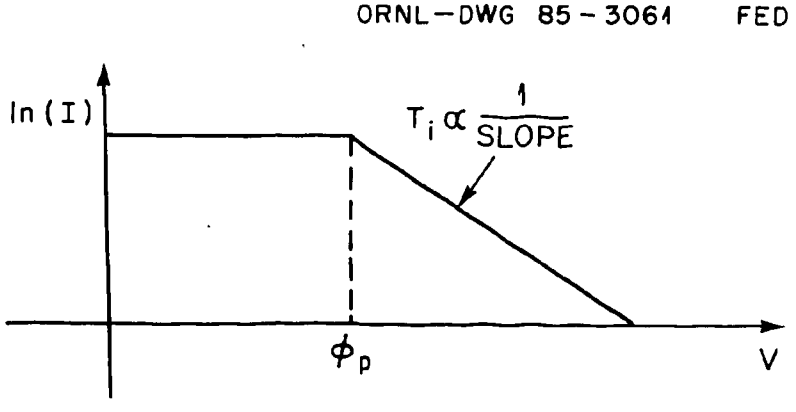

Fig. 3. The characteristic shape of end-loss analyzer (ELA) data for a simple mirror.

At the location of the ELA, the magnetic field is much smaller than in the plasma so that there is very little energy in cyclotron motion and the velocity is primarily along magnetic field lines. The total energy at the ELA can be rewritten as

$$E_T = 1/2mv_{\parallel}^2 + e\phi_p \ .$$

That the slope of the curve is inversely related to ion temperature comes from the Maxwellian nature of those particles lost through the loss cone. The constancy of the current until the ion repeller voltage reaches the peak potential value occurs because even zero-velocity particles gain a minimum energy of $e\phi_p$ as they fall out of the plasma.

An ELA can be used as a passive diagnostic on a tandem mirror but with some limitations. For example, no information can be obtained from the central cell when both ends of the central cell are electrostatically plugged; essentially no central-cell ions reach the ELA. The ELA can still measure the peak potential and ion temperature of the plug. Information about the central cell can be obtained if the tandem is operated in a single-ended mode, that is, only one plug operating as shown in Fig. 4. ELA 1 would provide plug ϕ_p and T_i; ELA 2 would provide central cell ϕ_e and T_i. It is assumed that the axial potential profile within the central cell is flat and that the ELA measurement of ϕ_e can accurately characterize the potential. On TMX a measurement of the axial potential at the central-cell midplane by an HIBP agreed with the ELA measurement.[5]

Detecting the thermal barrier potential requires active probing of the plasma with a diagnostic neutral beam and subsequent energy analysis of the beam particles by an ELA. As configured on TMX-U, the beam is aimed at a shallow angle to the machine axis and does not intercept the axis until the beam is in the region of the thermal barrier. The ELA looks along a flux tube centered on the machine axis. The spatial extent of the beam is comparable to the axial extent of the thermal barrier region, so alignment is critical. Beam neutrals that are ionized within the flux tube of an ELA placed at the opposite end of the tandem, as shown in Fig. 5, are detected by the ELA. Also shown is the characteristic $\ln(I)$ vs V curve.

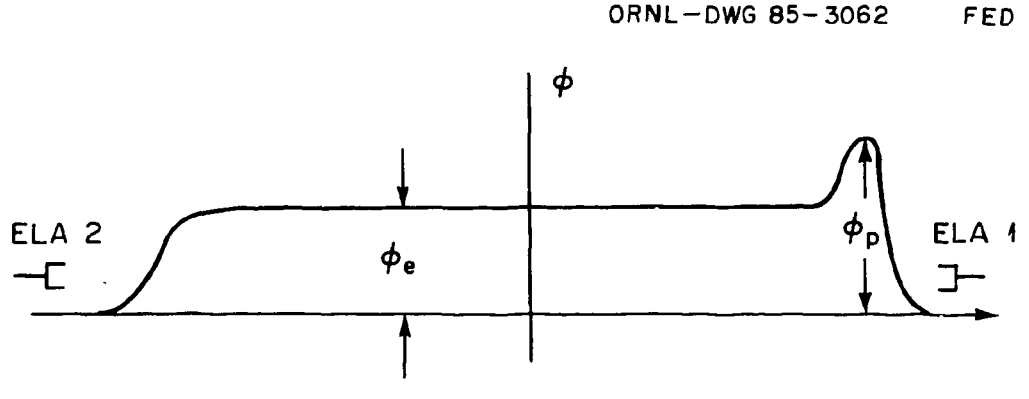

Fig. 4. Axial potential profile of a tandem mirror operating in a single-ended mode.

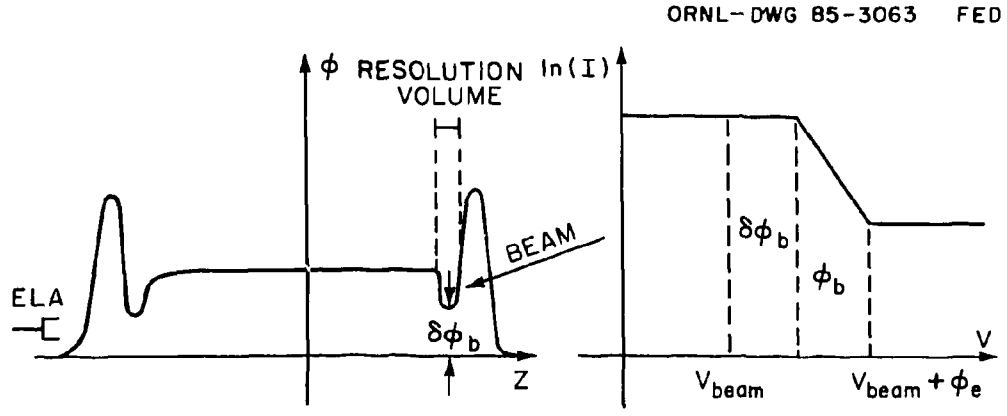

Fig. 5. ELA energy analysis of beam particles from a diagnostic neutral beam.

At the point of ionization, each beam ion behaves as a test particle. The spread in energy of these ions is a direct measure of the potential variation along the observed flux tube where they are created. The crossed-beam nature of the configuration uniquely defines the axial position of the measurement. The ELA is adjusted to sweep from just below the beam voltage (V_{beam}) to several kilovolts above it. As seen from Fig. 5, the first break in the curve occurs at voltage $V_{beam} + \delta\phi_b$, where $\delta\phi_b$ is the potential at the bottom of the thermal barrier. The second break in the curve occurs at the voltage $V_{beam} + \phi_c$, where ϕ_c is the central-cell potential. The difference in voltage between the two breaks is the barrier depth ϕ_b. Neutral beams do not have 100% of their output at the desired energy; some fraction is at one-half and one-third energy. On TMX-U, the ELA has been typically adjusted to examine the one-third energy component. A sample of actual TMX-U ELA data[6] from thermal barrier measurements is shown in Fig. 6. A 15-keV diagnostic neutral beam was used so that the one-third energy beam component was at 5 keV. On the Japanese thermal barrier tandem mirror, Gamma 10, the thermal barrier is formed in an axisymmetric simple mirror region. As a result, the HIBP is more suitable for potential measurements in the plug region. Measurements from Gamma 10's two HIBP systems, in the plug and central cell, are consistent with potential measurements on TMX-U.

4. DISCUSSION OF PUBLISHED DATA

This section illustrates data from two major tandem mirrors in the United States—TMX and TMX-U. Axial potential data from TMX[5,7] are shown in Fig. 7. High confidence is given to the axial location of the potential peaks because of measurements of the axial density profile and because of the relation of the axial density profile to the potential profile through the Boltzmann relation given in Sect. 2. The measurements were made by a combination of two techniques: an axial array of beam attenuation detectors to supply the relative density profile and a single-point, absolute density measurement by Thomson scattering to calibrate the profile. There is also high confidence in the ϕ_c measurement because the same value was obtained by an ELA and an HIBP when the device

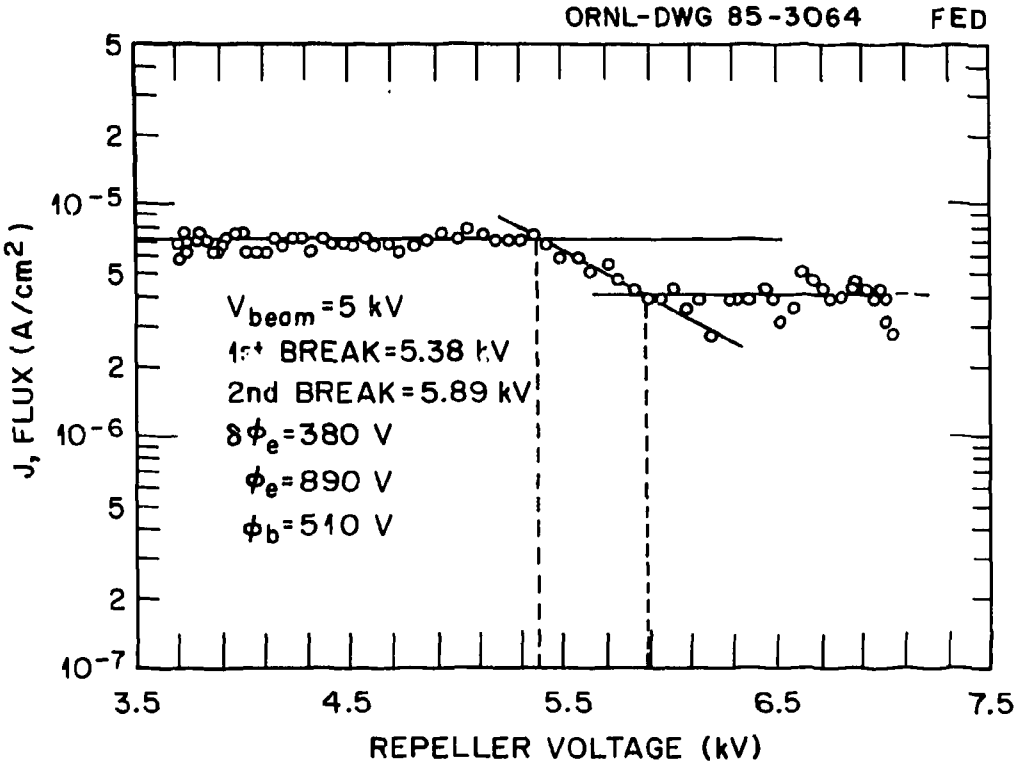

Fig. 6. Sample of actual active beam/ELA data from the TMX-U data base plotted as the natural logarithm of the detected current density vs repeller voltage. Listed are the results of the measurement.

was operated single endedly. TMX showed a plugging potential ϕ_p of about 500 V, a central-cell potential ϕ_e of about 400 V, and an ion confining potential ϕ_i of about 100 V.

Published data[8] for TMX-U claiming to show evidence for a thermal barrier are shown in Fig. 8, and, as illustrated, the device was run single endedly for this measurement. For completeness, Gamma 10 data[9] used for making the same claim and presented at a recent IAEA meeting are shown in Fig. 9. The Gamma 10 data are from experiments with both ends plugged. Only TMX-U data will be discussed further because the details of the experiments and measurements on Gamma 10 will be published shortly. There are a number of experimental ambiguities with the TMX data. First, the peak plugging potential could be stated only as a lower bound, as the maximum ELA 3 repeller bias (2.4 kV) was insufficient to repel any of the plasma ions escaping from the plug. Second, the HIBP was not operating reliably at this time to corroborate the measurement of ϕ_e, although the passive ELA 2 does provide the same number as the active beam/ELA 1 combination. For the experimental period ending in May 1985, double-ended experiments with an operating HIBP have provided ϕ_e measurements that are significantly lower than those provided by the active beam/ELA. The discrepancy may be caused by known calibration difficulties with the HIBP that only very recently appear to have been corrected. No new data from the HIBP have been taken. The axial potential profile may be as in Fig. 10.

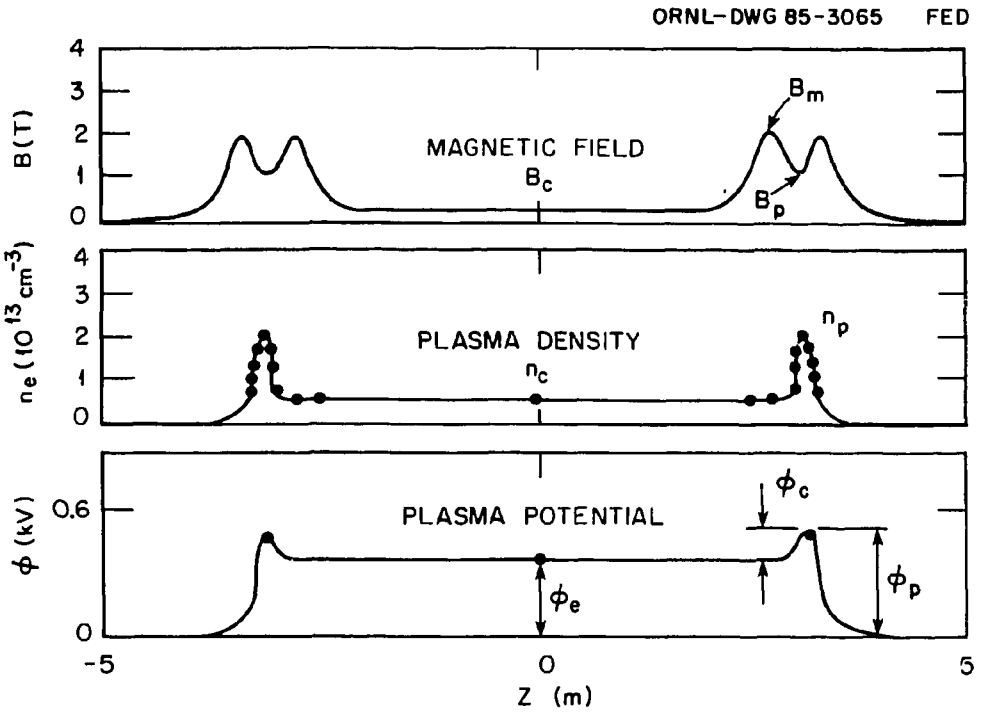

Fig. 7. Measured axial profiles of magnetic field, plasma density, and potential, shown to scale, for TMX.

Should recalibration not change the HIBP data, a reinterpretation of the active beam/ELA data is in order. Other interpretations have to do with the lack of knowing accurately where the measurement is being made. Recall that this method requires that the resolution volume be large enough to cover the predicted axial extent of the thermal barrier region. In addition, the resolution volume is fixed along the axis by the rigid mounting and aiming of the diagnostic neutral beam, so the data could be explained by an unanticipated axial shift of the desired profile or by a misalignment of the beam. The data could also be consistent with other entirely different and completely unexpected potential profiles that have nothing to do with alignment. Figure 11 is a schematic of the potential profile that highlights the present state of axial ambiguity with error bars in axial position for the measurements. It is clear that any number of profiles can be drawn through these points.

Another experimental difficulty is that there are no axial density profile measurements available for the plug during thermal barrier, strong end-plugging experiments. Thomson scattering does not work in the TMX-U plug as it did in TMX. There are some hardware difficulties, but the main reason is that the density there is much lower than in TMX. The lowest documented density measurement[10] by Thomson scattering (2×10^{11} cm^{-3}) is the level of expected density in the plug. This does not point out a problem with a thermal barrier tandem mirror because a goal of thermal barrier research is the

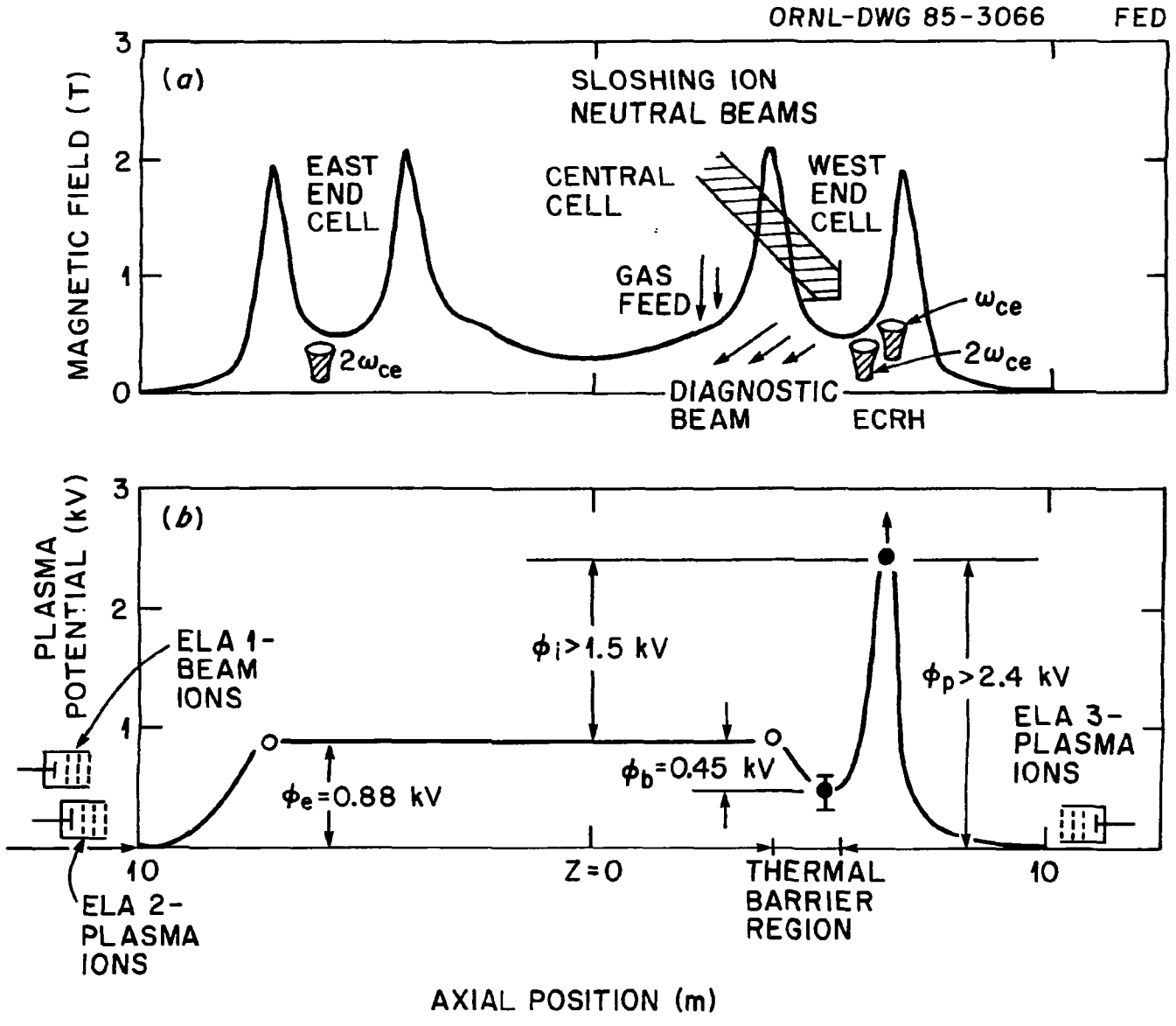

Fig. 8. Axial profiles of TMX-U (a) magnetic field and (b) expected potential profile during single-ended tandem operations including measured potentials (crosses). The measurements do not uniquely define the axial locations of ϕ_e or ϕ_p or the spatial variation of the potential in the barrier region.

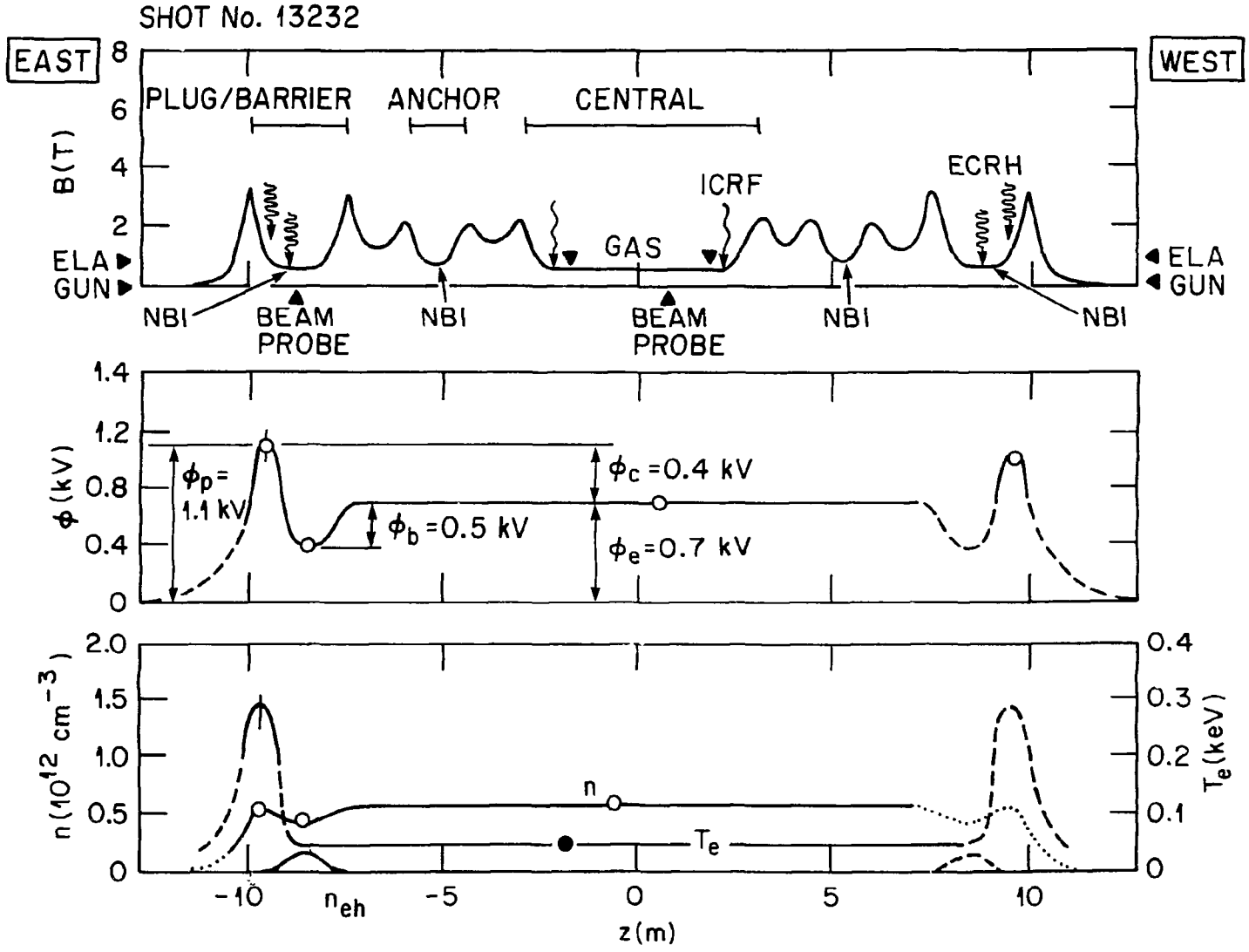

Fig. 9. Axial profiles of (top) magnetic field, (middle) potential, and (bottom) density and electron temperature in Gamma 10.

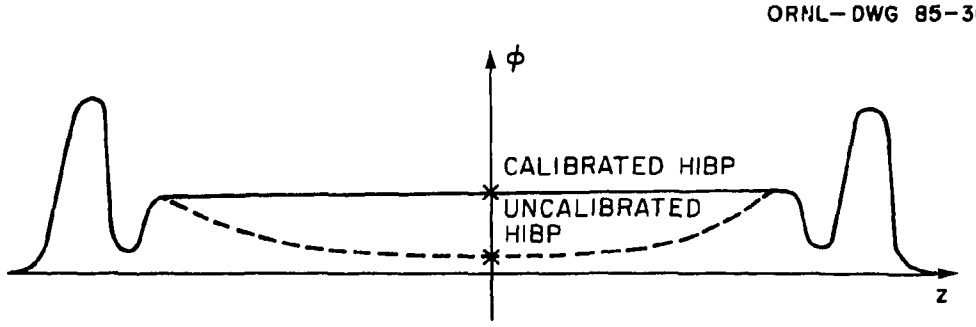

Fig. 10. Axial potential profiles for TMX-U, with and without HIBP recalibration. This assumes that recalibration produces the same value for ϕ_e as the ELA does.

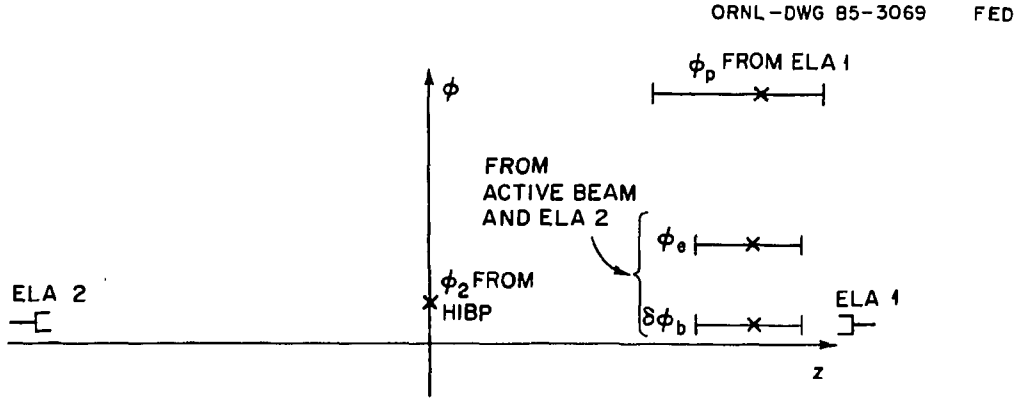

Fig. 11. Schematic diagram of the potential profile highlighting the present state of axial ambiguity of potential measurements.

ability to support a high-density central cell with a low-density plug. This is simply an experimental measurement problem.

Part of the resolution will come from a reliable, absolute calibration of the HIBP. Since Thomson scattering is difficult to do in the plug plasma, a microwave interferometer and an axial array of secondary emission detectors are being installed to obtain the axial density profile. In addition, the ELA used with the diagnostic neutral beam has been replaced by an end-loss ion spectrometer (ELIS[11]), a virtual copy of the $\mathbf{E}\|\mathbf{B}$ ion spectrometer built for the Tokamak Fusion Test Reactor (TFTR). This device does not require a swept voltage, so it can provide much better time resolution. This instrument is mass-sensitive and will be used together with gas puffing of trace gases into the plug plasma near the potential peak to determine the plug ϕ_p during strong thermal barrier end plugging. These improvements for better data and several others under way should provide for interesting physics debates over the weeks to come.

5. SUMMARY

In summary, this paper has outlined techniques to obtain one of the most fundamental measurements on a tandem mirror—the plasma potential. The techniques employed to measure axial potential for conventional and thermal barrier tandem mirrors have been discussed. Examples of typical data sets and their current interpretation have been discussed, together with plans for the future improvement of measurements of potential.

ACKNOWLEDGMENTS

This report was prepared for the U.S. Department of Energy, Office of Energy Research, Office of Fusion Energy, Division of Mirror Confinement Systems, while the author was temporarily assigned to that division for one year. The author wishes to thank Drs. Robert E. Price (DOE/OFE) and Thomas C. Simonen (LLNL) for their interest in and constructive review of this document.

REFERENCES

1. G. I. Dimov, V. V. Zakaidakov, and M. E. Kishinevskii, *Fiz. Plazmy* **2**, 597 (1976) [*Sov. J. Plasma Phys.* **2**, 326 (1976)]; T. K. Fowler and B. G. Logan, *Comments Plasma Phys. Controlled Fusion* **2**, 167 (1977).

2. D. E. Baldwin and B. G. Logan, "Improved Tandem Mirror Fusion Reactor," *Phys. Rev. Lett.* **43**, 105 (1979).

3. A. W. Molvik, "Large Acceptance Angle Retarding-Potential Analyzers," *Rev. Sci. Instrum.* **52**, 704 (1981).

4. T. D. Rognlien and T. A. Cutler, "Transition from Patunkov to Collisional Confinement in a Magnetic Electrostatic Well," *Nucl. Fusion* **20**, 1003 (1980).

5. D. L. Correll et al., "Ambipolar Potential Formation and Axial Confinement in TMX," *Nucl. Fusion* **22**, 223 (1982).

6. T. C. Simonen, Lawrence Livermore National Laboratory, Livermore, Calif., personal communication, May 1985.

7. T. C. Simonen, "Comparison of TMX Tandem Mirror Confinement with Single-Mirror Experiments," *Nucl. Fusion* **21**, 1667 (1981).

8. D. P. Grubb et al., "Thermal-Barrier Production and Identification in a Tandem Mirror," *Phys. Rev. Lett.* **53**, 783 (1984).

9. T. Cho et al., "Potential Formation in Axisymmetrized Tandem Mirror Gamma 10," Paper IAEA-CN-44/C-I-3 in *Proceedings of the 10th International Conference on Plasma Physics and Controlled Nuclear Fusion Research (London, 1984)*, vol. 1, IAEA, Vienna, 1985.

10. J. A. Cobble, "Thomson Scattering at Plasma Densities Below 10^{12} cm^{-3}," *Rev. Sci. Instrum.* **56**, 73 (1985).

11. J. H. Foote et al., *The E‖B End-Loss-Ion Analyzer for TMX-U*, UCRL-91270, University of California, Lawrence Livermore Natl. Lab., Livermore, Calif., September 1984.

ORNL/TM-9705
Dist. Category UC-20

INTERNAL DISTRIBUTION

1. F. W. Baity
2. D. B. Batchelor
3. R. J. Colchin
4. R. A. Dory
5. J. L. Dunlap
6–9. J. C. Glowienka
10. G. R. Haste
11. C. L. Hedrick
12. D. L. Hillis
13. S. Hiroe
14. E. A. Lazarus
15. G. H. Neilson
16. L. W. Owen
17. R. K. Richards
18. D. A. Rasmussen
19. M. J. Saltmarsh
20. D. W. Swain
21. C. E. Thomas
22. N. A. Uckan
23. T. Uckan
24. T. L. White
25. J. B. Wilgen
26. J. Sheffield
27–28. Laboratory Records Department
29. Laboratory Records, ORNL-RC
30. Document Reference Section
31. Central Research Library
32. Fusion Energy Division Library
33–34. Fusion Energy Division Publications Office
35. ORNL Patent Office

EXTERNAL DISTRIBUTION

36. Office of the Assistant Manager for Energy Research and Development, Department of Energy, Oak Ridge Operations, Box E, Oak Ridge, TN 37831
37. J. D. Callen, Department of Nuclear Engineering, University of Wisconsin, Madison, WI 53706
38. R. W. Conn, Department of Chemical, Nuclear, and Thermal Engineering, University of California, Los Angeles, CA 90024
39. S. O. Dean, Director, Fusion Energy Development, Science Applications, International Corporation, Research Park, 230 Wall Street, Gaithersburg, MD 20879
40. H. K. Forsen, Bechtel Group, Inc., Research Engineering, P.O. Box 3965, San Francisco, CA 94105
41. J. R. Gilleland, GA Technologies, Inc., Fusion and Advanced Technology, P.O. Box 85608, San Diego, CA 92138
42. R. W. Gould, Department of Applied Physics, California Institute of Technology, Pasadena, CA 91125
43. R. A. Gross, Plasma Research Laboratory, Columbia University, New York, NY 10027

44. D. M. Meade, Princeton Plasma Physics Laboratory, P.O. Box 451, Princeton, NJ 08544
45. W. M. Stacey, Jr., School of Mechanical Engineering, Georgia Institute of Technology, Atlanta, GA 30332
46. D. Steiner, Nuclear Engineering Department, NES Building, Tibbetts Avenue, Rensselaer Polytechnic Institute, Troy, NY 12181
47. R. Varma, Physical Research Laboratory, Navrangpura, Ahmedabad 380009, India
48. Bibliothek, Max-Planck Institut fur Plasmaphysik, D-8046 Garching, Federal Republic of Germany
49. Bibliothek, Institut fur Plasmaphysik, KFA, Postfach 1913, D-5170 Julich, Federal Republic of Germany
50. Bibliotheque, Centre de Recherches en Physique des Plasmas, 21 Avenue des Bains, 1007 Lausanne, Switzerland
51. Bibliotheque, Service du Confinement des Plasmas, CEA, B.P. 6, 92 Fontenay-aux-Roses (Seine), France
52. Documentation S.I.G.N., Departement de la Physique du Plasma et de la Fusion Controlee, Centre d'Etudes Nucleaires, B.P. No. 85, Centre du Tri, 38041 Cedex, Grenoble, France
53. Library, Culham Laboratory, UKAEA, Abingdon, Oxfordshire, OX14 3DB, England
54. Library, FOM-Instituut voor Plasma-Fysica, Rijnhuizen, Edisonbaan 14, 3439 MN Nieuwegein, The Netherlands
55. Library, Institute of Plasma Physics, Nagoya University, Nagoya 64, Japan
56. Library, International Centre for Theoretical Physics, Trieste, Italy
57. Library, Laboratorio Gas Ionizzati, CP 56, I-00044 Frascati (Roma), Italy
58. Library, Plasma Physics Laboratory, Kyoto University, Gokasho, Uji, Kyoto, Japan
59. Plasma Research Laboratory, Australian National University, P.O. Box 4, Canberra, A.C.T. 2000, Australia
60. Thermonuclear Library, Japan Atomic Energy Research Institute, Tokai-mura, Ibaraki Prefecture, Japan
61. R. A. Blanken, Office of Fusion Energy, Office of Energy Research, ER-542, Germantown, U.S. Department of Energy, Washington, DC 20545
62. K. Bol, Princeton Plasma Physics Laboratory, P.O. Box 451, Princeton, NJ 08544
63. R. A. E. Bolton, IREQ Hydro-Quebec Research Institute, 1800 Montee Ste.-Julie, Varennes, P.Q. JOL 2P0, Canada
64. R. L. Freeman, GA Technologies, Inc., Fusion and Advanced Technology, P.O. Box 85608, San Diego, CA 92138
65. K. W. Gentle, RLM 11.222, Institute for Fusion Studies, University of Texas, Austin, TX 78712
66. R. J. Goldston, Princeton Plasma Physics Laboratory, P.O. Box 451, Princeton, NJ 08544
67. J. C. Hosea, Princeton Plasma Physics Laboratory, P.O. Box 451, Princeton, NJ 08544
68. S. W. Luke, Office of Fusion Energy, Office of Energy Research, ER-55, Germantown, U.S. Department of Energy, Washington, DC 20545

69. E. Oktay, Office of Fusion Energy, Office of Energy Research, ER-55, Germantown, U.S. Department of Energy, Washington, DC 20545
70. D. Overskei, GA Technologies, Inc., Fusion and Advanced Technology, P.O. Box 85608, San Diego, CA 92138
71. R. R. Parker, MIT Plasma Fusion Center, 167 Albany Street, Cambridge, MA 02139
72. W. L. Sadowski, Office of Fusion Energy, Office of Energy Research, ER-541, Germantown, U.S. Department of Energy, Washington, DC 20545
73. J. W. Willis, Office of Fusion Energy, Office of Energy Research, ER-55, Germantown, U.S. Department of Energy, Washington, DC 20545
74. A. P. Navarro, Division de Fusion, Junta de Energia Nuclear, Avenida Complutense 22, Madrid (3), Spain
75. Laboratory for Plasma and Fusion Studies, Department of Nuclear Engineering, Seoul National University, Shinrim-dong, Gwanak-ku, Seoul 151, Korea
76–80. R. E. Price, Office of Fusion Energy, ER-55, Office of Energy Research, U.S. Department of Energy: GTN, Washington, DC 20545
81. J. F. Clarke, Office of Fusion Energy ER-50, Office of Energy Research, U.S. Department of Energy: GTN, Washington, DC 20545
82. N. A. Davies, Office of Fusion Energy ER-51, Office of Energy Research, U.S. Department of Energy: GTN, Washington, DC 20545
83. J. M. Turner, Office of Fusion Energy ER-52, Office of Energy Research, U.S. Department of Energy: GTN, Washington, DC 20545
84–88. T. C. Simonen, L-637, Lawrence Livermore National Laboratory, P.O. Box 5511, Livermore, CA 94550
89. T. K. Fowler, L-640, Lawrence Livermore National Laboratory, P.O. Box 5511, Livermore, CA 94550
90. D. Baldwin, L-630, Lawrence Livermore National Laboratory, P.O. Box 5511, Livermore, CA 94550
91. G. A. Eliseev, I. V. Kurchatov Institute of Atomic Energy, P.O. Box 3402, 123182 Moscow, U.S.S.R.
92. V. A. Glukhikh, Scientific-Research Institute of Electro-Physical Apparatus, 188631 Leningrad, U.S.S.R.
93. I. Shpigel, Institute of General Physics, Academy of Sciences, Ulitsa Vavilova 38, Moscow, U.S.S.R.
94. D. D. Ryutov, Institute of Nuclear Physics, Siberian Branch of the Academy of Sciences of the U.S.S.R., Sovetskaya St. 5, 630090 Novosibirsk, U.S.S.R.
95. V. T. Tolok, Kharkov Physical-Technical Institute, Academical St. 1, 310108 Kharkov, U.S.S.R.
96. Library, Institute of Physics, Academia Sinica, Beijing, Peoples' Republic of China
97–204. Given distribution according to TIC-4500, Magnetic Fusion Energy (Distribution Category UC-20)

ABSTRACT

The U.S. mirror program has begun conducting experiments with a thermal barrier tandem mirror configuration. This configuration requires a specific axial potential profile and implies measurements of potential for documentation and optimization of the configuration. This report briefly outlines the motivation for the thermal barrier tandem mirror and then outlines the techniques used to document the potential profile in conventional and thermal barrier tandem mirrors. Examples of typical data sets from the world's major tandem mirror experiments, TMX and TMX-U at Lawrence Livermore National Laboratory (LLNL) and Gamma 10 at Tsukuba University in Japan, and the current interpretation of the data are discussed together with plans for the future improvement of measurements of plasma potential.